Spin-Wave Interference in Three-Dimensional Rolled-Up Ferromagnetic Microtubes

Felix Balhorn, Sebastian Mansfeld, Andreas Krohn, Jesco Topp, Wolfgang Hansen, Detlef Heitmann, and Stefan Mendach*

Institut für Angewandte Physik und Zentrum für Mikrostrukturforschung, Universität Hamburg, Jungiusstrasse 11, D-20355 Hamburg, Germany

(Received 14 August 2009; revised manuscript received 2 October 2009; published 21 January 2010)

We have investigated spin-wave excitations in rolled-up Permalloy microtubes using microwave absorption spectroscopy. We find a series of quantized azimuthal modes which arise from the constructive interference of Damon-Eshbach-type spin waves propagating around the circumference of the microtubes, forming a spin-wave resonator. The mode spectrum can be tailored by the tube's radius and number of rolled-up layers.

DOI: 10.1103/PhysRevLett.104.037205 PACS numbers: 75.40.Gb, 75.75.−c, 76.50.+g, 81.16.Dn

Spin-wave excitations in thin films and patterned ferromagnetic structures are of both fundamental and practical scientific interest. On the micrometer scale, geometric boundaries induce quantization conditions on spin-wave excitations. This effect has been shown for flat laterally patterned geometries such as wires and rectangular elements [1,2] as well as for micrometer sized rings and discs [3–6].

In this Letter, we report on the fabrication and experimental investigation of novel three-dimensional ferromagnetic microstructures consisting of rolled-up Permalloy-semiconductor ($Ni_{80}Fe_{20}/GaAs/In_{20}Ga_{80}As$) layers which, in the following, are termed rolled-up Permalloy microtube (RUPT). Using microwave absorption spectroscopy on homogeneously magnetized RUPTs, we observe a series of sharp modes which arise from the constructive interference of Damon-Eshbach-type [7] spin waves traveling along the circumference of the RUPT. These interference conditions are quite universal. They resemble the acoustic whispering-gallery modes in St. Paul's Cathedral, originally explored by Lord Rayleigh [8], optical resonators based on semiconductor microtubes [9,10], and microdiscs or dielectric microspheres [11].

The measurements discussed in this work were performed on two RUPTs with different radii r, winding numbers N (giving the number of revolutions of the rolled-up material), and layer composition (RUPT A and RUPT B, with parameters given below). They were prepared from a strained Permalloy-semiconductor multilayer, utilizing the self-rolling effect [12] pioneered by Prinz *et al.* [13] and Schmidt *et al.* [14].

For RUPT A (RUPT B), a $t = 20$ nm thick Permalloy layer was thermally evaporated on a molecular beam epitaxy grown heterostructure made of 15 nm (10 nm) GaAs, 15 nm pseudomorphically strained $In_{20}Ga_{80}As$, and a 40 nm AlAs sacrificial layer on a GaAs substrate [see Fig. 1(a)]. By selectively etching the AlAs sacrificial layer, the $Ni_{80}Fe_{20}/GaAs/In_{20}Ga_{80}As$ layer system is released from the substrate and minimizes its strain energy by rolling up into a tube [see Figs. 1(b) and 1(c)]. The diameter d of the RUPT is determined by the composition and thickness of the $Ni_{80}Fe_{20}/GaAs/In_{20}Ga_{80}As$ layer system [15]. The length l and winding number N of the RUPT can be precisely controlled by photolithography, i.e., by defining the lateral dimensions of a strained mesa which is rolled up in the final selective etching step from a well-defined starting edge [16]. After measurements, the quality of the multilayered walls of the RUPTs was monitored with focused ion beam cross sections as exemplarily shown in the inset of Fig. 1(c) for RUPT A, which exhibits a tightly wound spiral shape with 3.5 windings. Together with each RUPT, an unpatterned Permalloy film was prepared on the same wafer, using the same thermal evaporation step to

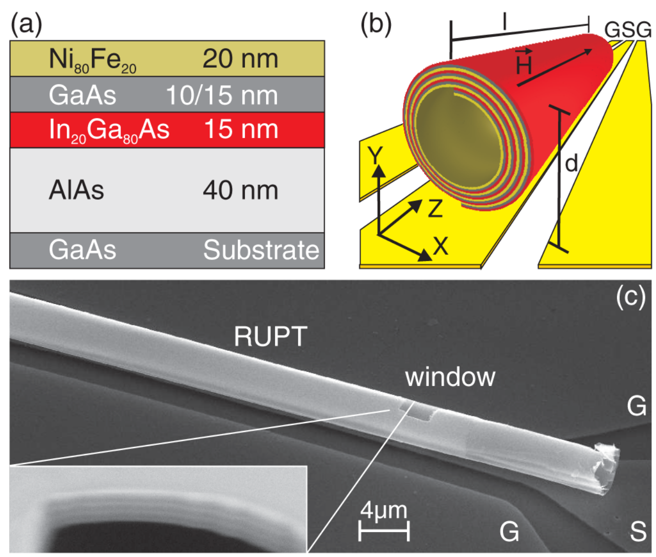

FIG. 1 (color online). (a) Layer sequence used to roll up a strained $Ni_{80}Fe_{20}/GaAs/In_{20}Ga_{80}As$ layer system into a Permalloy microtube (RUPT). (b) Sketch of a RUPT positioned on the signal line (S) between the two ground lines (G) of a coplanar waveguide to perform microwave absorption measurements. (c) SEM image of RUPT A corresponding to the scheme in (b). The inset shows 3.5 tight windings of the strained layer system in a tube cross section drilled by focused ion beams after the measurements were performed.

allow the determination of reference parameters. The film for RUPT A (RUPT B) has a saturation magnetization $\mu_0 M_s = 980$ mT ($\mu_0 M_s = 1080$ mT) and a Gilbert damping constant $\alpha = 0.008$ ($\alpha = 0.008$), as determined by microwave absorption measurements.

We investigated the spin-wave spectrum using high-resolution microwave absorption spectroscopy. For this purpose, the RUPT was removed from the GaAs substrate and placed on the 2.4 μm wide signal line of a coplanar waveguide (CPW) using a setup with piezo-controlled manipulation needles [17]. The CPW was defined by optical lithography on a GaAs wafer and consists of a 170 nm thick trilayer of Cr/Ag/Au. A static external magnetic field $\vec{H}$ was applied in the plane of the waveguide. With a vector network analyzer (VNA), we measured the microwave transmission through the CPW in dependence of the microwave frequency f. The high-frequency magnetic field of the CPW $h(x, y)$ pointed perpendicularly to the axis of the RUPT. The excitation of a spin wave is indicated by a reduced transmission of the waveguide due to the absorption of power at the corresponding excitation frequency f. Each measurement was normalized to a reference measurement, taken with $\mu_0 H_{\mathrm{ref}} = 90$ mT applied perpendicularly to the axis of the RUPT. To assure a well-defined magnetization configuration within the RUPT, it was magnetized along its axis with $\mu_0 H_1 = 50$ mT prior to every frequency sweep. The magnetic field was then ramped down to zero and finally ramped up to the actual field value.

Let us first discuss measurements performed on RUPT A with diameter $d_A = 3.5$ μm, length $l_A = 60$ μm, and rolling number $N_A = 3.5$. Figure 2(a) shows the excitation spectrum of RUPT A at an external magnetic field $H = 0$. Four distinct resonances are observed at $f_{A,0} = 3.5$ GHz, $f_{A,1} = 4.5$ GHz, $f_{A,2} = 5.3$ GHz, and $f_{A,3} = 5.8$ GHz. With increasing external magnetic field, the spacing between all resonance peaks reduces until they overlap. To determine the exact eigenfrequency of each spin wave, each peak was fitted assuming a Lorentzian shaped curve. Figure 2(b) depicts a plot of the resonance frequency of the three larger resonance peaks for different external magnetic fields H. Figures 2(c) and 2(d) display corresponding data for RUPT B with diameter $d_A = 2.8$ μm, length $l_A = 100$ μm, and winding number $N_B = 1.8$. This RUPT shows four resonance peaks for $H = 0$ at $f_{B,0} = 4.1$ GHz, $f_{B,1} = 5.1$ GHz, $f_{B,2} = 6.1$ GHz, and $f_{B,3} = 6.7$ GHz. RUPT B absorbs about twice as much microwave power as RUPT A.

In the following, we show that the resonances in the spectra of RUPT A and RUPT B are due to spin waves traveling around the RUPT's perimeter. They form resonant modes $n = 0, 1, 2, 3, \ldots$ if the periodic boundary condition for a ring resonator

$$n\lambda = \pi d \Leftrightarrow k_\phi = 2n/d, \qquad n \epsilon \mathbb{N}_0 \tag{1}$$

is fulfilled. Here λ denotes the wavelength of the spin wave, k_ϕ the azimuthal wave vector, and d the diameter of the RUPT. Condition (1) is true if an integer number of wavelengths fits into the circumference of the RUPT, so that spin waves interfere constructively. We prepared RUPT B on purpose with smaller diameter and a winding number of only 1.8 to confirm our explanation. The fact that we observe four resonant modes for RUPT B as well confirms that they originate from interfering azimuthal spin waves and not from individual isolated modes in single films or parts of the circumference. In particular, we observe that with decreasing diameter $d = 2.8$ μm for RUPT B, as compared to $d = 3.5$ μm for RUPT A, the resonance frequency increases as expected from the spin-wave model described below.

At first it seems surprising that spin waves interfere on the circumference, since the actual ferromagnetic film is of spiral and not closed shape. The explanation is that the

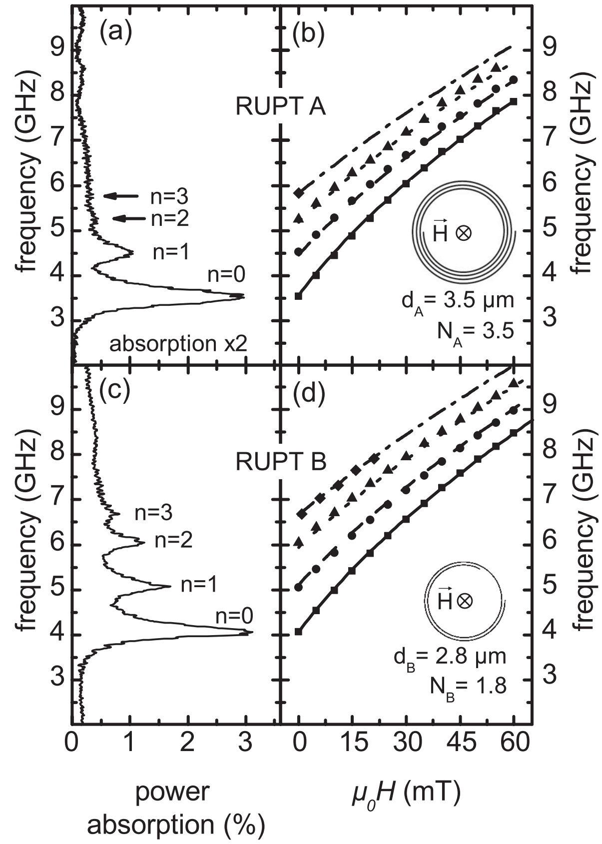

FIG. 2. (a) and (c) show microwave power absorption spectra at $H = 0$ for RUPT A and RUPT B, respectively. In both cases, four successive resonances corresponding to azimuthal spin-wave modes with number $n = 0$, 1, 2, and 3 can be identified. (b) and (d) show the magnetic field dependence of the measured resonance frequency peaks indicated by symbols for RUPT A and RUPT B, respectively, in very good agreement with the corresponding theory curves calculated with our spin-wave interference model ($n = 0$: ■, continuous curve; $n = 1$: ●, dashed curve; $n = 2$: ▲, dotted curve; $n = 3$: ◆, dash-dotted curve). As indicated, the magnetic field points along the tube axis.

individual overlapping films couple strongly through dipole-dipole interaction. This coupling also automatically leads to a renormalization of the spin-wave mode frequencies as compared to a single-layered film. This can be modeled by a single-layered tube with an effective thickness t_{eff}. Additionally, the curved shape of the microtubes also leads to both static and dynamic demagnetization effects [17]. This—the demagnetization—coupling and renormalization and their incorporation into a spin-wave model will be addressed in detail in the following.

Spin-wave model.—To describe our data, we start from a model introduced by Kalinikos and Slavin [18] for a flat thin film, modified by Guslienko *et al.* [19]. This approach was used before to describe spin-wave resonances in flat Permalloy rings with in-plane external magnetic field. Except for the zero magnetic field case [20], the spin-wave dispersion exhibits a complex radial and azimuthal dependence in these flat Permalloy rings, and resonance conditions are only met up to a certain magnetic field [5]. In contrast to this, here, spin waves traveling around the perimeter of an axially magnetized RUPT with an external magnetic field parallel to its axis exhibit the same dispersion in the entire RUPT enabling azimuthal resonances for all magnetic field values over a broad spectral range. This Damon-Eshbach-type dispersion is plotted in Fig. 3 and given by

$$f(k_\phi, H_{\mathrm{int}}) = \frac{\gamma\mu_0}{2\pi}\sqrt{\left[H_{\mathrm{int}} + \frac{2A}{(\mu_0 M_s)}k_\phi^2\right]} \cdot \sqrt{\left[H_{\mathrm{int}} + \frac{2A}{(\mu_0 M_s)}k_\phi^2 + M_s F(k_\phi, H_{\mathrm{int}})\right]}. \tag{2}$$

H_{int} is the internal magnetic field, A is the exchange constant for Permalloy ($A = 13 \times 10^{-12} \frac{J}{m}$), M_s is the saturation magnetization, and $F(k_\phi, H_{\mathrm{int}})$ is the dipole-dipole interaction matrix given by

$$F(k_\phi, H_{\mathrm{int}}) = 1 + P(k_\phi)[1 - P(k_\phi)]\left(\frac{M_s}{H_{\mathrm{int}} + \frac{2A}{(\mu_0 M_s)}k_\phi^2}\right), \tag{3}$$

with $P(k_\phi) = 1 - \frac{1-e^{-k_\phi t_{\mathrm{eff}}}}{k_\phi t_{\mathrm{eff}}}$. From the quantized wave vector k_ϕ defined in Eq. (1), we directly get the corresponding resonance frequency. In Fig. 3 we see that indeed the spacing between the modes decreases with mode number as observed in the experiment. We used this model to fit our data. The coupling and frequency renormalization were accounted for by an effective layer thickness t_{eff}. As explained below, the demagnetization was considered by adding an effective demagnetizing field to the internal magnetic field, $H_{\mathrm{int}} = H + H_{\mathrm{dem}}$. We find a nearly perfect agreement with the experimental data using $t_{\mathrm{eff}} = 37$ nm and $\mu_0 H_{\mathrm{dem}} = 16$ mT for RUPT A and $t_{\mathrm{eff}} = 30$ nm and $\mu_0 H_{\mathrm{dem}} = 20$ mT for RUPT B. The fit is shown in Figs. 2(b) and 2(d).

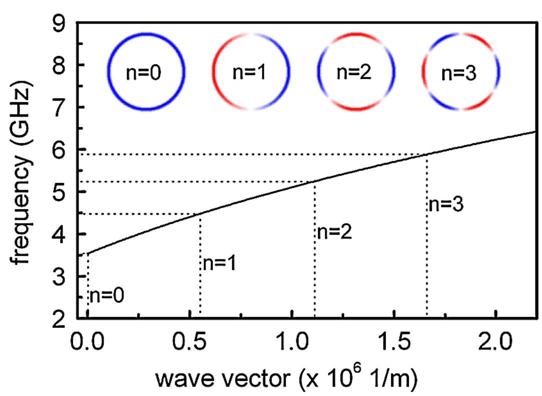

FIG. 3 (color online). Calculated magnetic dispersion for RUPT A at $H = 0$ with an effective thickness $t_{\mathrm{eff}} = 37$ nm and an effective demagnetizing field of $\mu_0 H_{\mathrm{dem}} = 16$ mT. The dotted lines mark the wave vector for modes $n = 0$, 1, 2, and 3 and the corresponding resonant frequencies. The inset color plots show the phase distribution in the RUPT for $n = 0$, 1, 2, and 3 [red (light gray) and blue (gray) represent opposite phase].

Demagnetization.—Because of the bent shape of the RUPT, any precession of the magnetization leads to magnetization components pointing towards geometric boundaries. This causes dynamic demagnetizing effects which form a two-dimensional potential energy landscape for a precessing spin [17]. For this reason, even for $H = 0$, the RUPT has a resonance frequency $f \neq 0$. Thus, to explain our data we have to take into account an additional effective demagnetizing field H_{dem}. This concept is similar to the treatment of a thin ferromagnetic wire in the Kittel formula [21]. For wires, such an effective field can be accurately retrieved from the hard-axis dispersion relation, i.e., when the external field and the long axis of the wire are perpendicular to each other. At the external field for which the frequency of the fundamental spin-wave mode is minimal, the external and the demagnetization field compensate each other [22]. Using this value for H_{dem}, the resonance frequency and dispersion of a thin wire can be modeled within sufficient accuracy. We used an identical approach for the RUPTs. The experimentally observed hard-axis dispersion indeed displays a pronounced minimum at $\mu_0 H = 17$ mT for RUPT A and at $\mu_0 H = 21$ mT for RUPT B [see Figs. 4(a) and 4(b)]. These values are quite close to the values $\mu_0 H_{\mathrm{dem}} = 16$ mT for RUPT A and $\mu_0 H_{\mathrm{dem}} = 20$ mT for RUPT B obtained independently from fitting our data with our model as described above and shown in Fig. 2.

Dipole coupling.—The RUPT is of spiral shape so that at first sight there is no periodic azimuthal path through ferromagnetic material for the spin waves to travel. Instead, the spin waves traveling in individual layers of the RUPT couple via dipole-dipole interaction. To support this approach, we performed micromagnetic simulations using the OOMMF framework [23]. The simulation of the bent shape of a microtube is, however, extremely time consuming and beyond our computer capacities due to

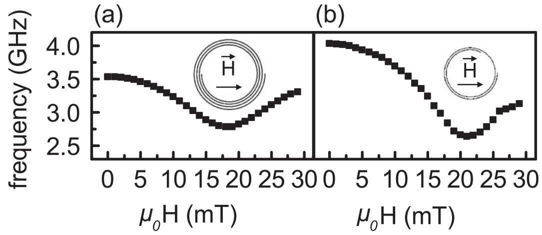

FIG. 4. (a) and (b) show the hard-axis magnetic field dependence of the $n = 0$ resonance frequency for RUPT A and RUPT B, respectively. In both cases, the resonance frequency reaches a minimum, from which we can extract the absolute value of the effective demagnetizing field H_{dem}.

the rectangular discretization of space required for the simulations with OOMMF. Instead, we simulated two thin rectangular Permalloy stripes stacked vertically (separation distance 35 nm). Only the lower stripe is excited directly by a 2.6 ps long pulse applied perpendicularly to an external in-plane field of 20 mT. Our simulations show that the second not directly excited stripe follows the excitation of the lower stripe via dipole-dipole coupling with almost the same amplitude, indeed indicating strong dipole-dipole coupling.

Renormalization.—Because of the coupling, the spin excitations can be treated as a one-layered spin-wave system, described by an effective thickness. As discussed above, we find a nearly perfect agreement using an effective thickness of $t_{\mathrm{eff}} = 37$ nm (30 nm) for RUPT A (B). These values lie in between the thickness of a single layer, $t = 20$ nm, and the total thickness of 80 nm (40 nm) for RUPT A (B). Also in the micromagnetic simulations, we find that the resonance frequency of the coupled two-layered stripe system is shifted to higher frequencies with regard to the single-layered system, which can indeed be described by an increased effective thickness.

In conclusion, we have fabricated and investigated novel ferromagnetic microtube ring resonators. We observe quantized spin-wave modes arising from the constructive interference on the circumference of the tube. The zero magnetic field mode spectrum can be tailored by the tube's radius and number of windings. The homogeneous magnetization in our rolled-up structures resembles the refractive index in optical resonators (e.g., [9]) or the stiffness in acoustic materials and can be tuned simply by changing the external magnetic field. Our rolled-up structures exhibit well separated sharp whispering-gallery modes, which exist over a broad magnetic field range and can be tuned over several GHz. In this way, our microtube ring resonators open a wide field of fundamental research and practical applications.

We would like to thank Markus Bröll, Stephan Schwaiger, and Yuliya Stark for help during the tube preparation and Jan Podbielski and Dirk Grundler for fruitful discussions. We acknowledge financial support by the DFG via Grants No. SFB 668, No. SFB 508, and GrK 1286, as well as by the Cluster of Excellence "Nano-Spintronics."

Note added in proof.—Recently, the authors of Ref. [24] reported on spin wave interference in rectangular $Co_{90}Zr_5Ta_5$ tubes.

*Corresponding author.
smendach@physnet.uni-hamburg.de

[1] J. Jorzick, S. O. Demokritov, B. Hillebrands, M. Bailleul, C. Fermon, K. Y. Guslienko, A. N. Slavin, D. V. Berkov, and N. L. Gorn, Phys. Rev. Lett. **88**, 047204 (2002).
[2] C. Bayer, J. P. Park, H. Wang, M. Yan, C. E. Campbell, and P. A. Crowell, Phys. Rev. B **69**, 134401 (2004).
[3] J. Jorzick, S. O. Demokritov, B. Hillebrands, B. Bartenlian, C. Chappert, D. Decanini, F. Rousseaux, and E. Cambril, Appl. Phys. Lett. **75**, 3859 (1999).
[4] J. P. Park and P. A. Crowell, Phys. Rev. Lett. **95**, 167201 (2005).
[5] J. Podbielski, F. Giesen, and D. Grundler, Phys. Rev. Lett. **96**, 167207 (2006).
[6] I. Neudecker, M. Klaui, K. Perzlmaier, D. Backes, L. J. Heyderman, C. A. F. Vaz, J. A. C. Bland, U. Rudiger, and C. H. Back, Phys. Rev. Lett. **96**, 057207 (2006).
[7] R. W. Damon and J. R. Eshbach, J. Phys. Chem. Solids **19**, 308 (1961).
[8] L. Rayleigh, Philos. Mag. **20**, 1001 (1910).
[9] C. Strelow, H. Rehberg, C. M. Schultz, H. Welsch, C. Heyn, D. Heitmann, and T. Kipp, Phys. Rev. Lett. **101**, 127403 (2008).
[10] S. Mendach, S. Kiravittaya, A. Rastelli, M. Benyoucef, R. Songmuang, and O. G. Schmidt, Phys. Rev. B **78**, 035317 (2008).
[11] K. J. Vahala, Nature (London) **424**, 839 (2003).
[12] A. Cho, Science **313**, 164 (2006).
[13] V. Y. Prinz, V. A. Seleznev, A. K. Gutakovsky, A. V. Chehovskiy, V. V. Preobrazhenskii, M. A. Putyato, and T. A. Gavrilova, Physica (Amsterdam) **6E**, 828 (2000).
[14] O. G. Schmidt and K. Eberl, Nature (London) **410**, 168 (2001).
[15] M. Grundmann, Appl. Phys. Lett. **83**, 2444 (2003).
[16] O. Schumacher, S. Mendach, H. Welsch, A. Schramm, C. Heyn, and W. Hansen, Appl. Phys. Lett. **86**, 143109 (2005).
[17] S. Mendach, J. Podbielski, J. Topp, W. Hansen, and D. Heitmann, Appl. Phys. Lett. **93**, 262501 (2008).
[18] B. A. Kalinikos and A. N. Slavin, J. Phys. C **19**, 7013 (1986).
[19] K. Y. Guslienko, R. W. Chantrell, and A. N. Slavin, Phys. Rev. B **68**, 024422 (2003).
[20] F. Hoffmann, G. Woltersdorf, K. Perzlmaier, A. N. Slavin, V. S. Tiberkevich, A. Bischof, D. Weiss, and C. H. Back, Phys. Rev. B **76**, 014416 (2007).
[21] C. Kittel, Phys. Rev. **73**, 155 (1948).
[22] M. Bailleul, D. Olligs, and C. Fermon, Phys. Rev. Lett. **91**, 137204 (2003).
[23] M. Donahue and D. G. Porter, National Institute of Standards and Technology Interagency Report NISTIR 6376, 1999, http://math.nist.gov/oommf/.
[24] A. Kozhanov, D. Ouellette, M. Rodwell, D. W. Lee, S. X. Wang, and S. J. Allen, IEEE Trans. Magn. **45**, 4223 (2009).